Asian Journal of Chemistry; Vol. 26, Supplementary Issue (2014), S73-S76

ASIAN JOURNAL OF CHEMISTRY

http://dx.doi.org/10.14233/ajchem.2014.19016

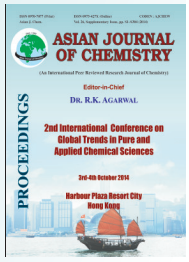

Cyclic Microwave-Modified Sol-Gel Process of $NaY(WO_4)_2$:Ho^{3+}/Yb^{3+} Phosphors and Their Upconversion Photoluminescence Properties

CHANG SUNG LIM

Department of Advanced Materials Science and Engineering, Hanseo University, Seosan 356-706, Republic of Korea

Corresponding author: Tel/Fax: +82 41 6601445; E-mail: cslim@hanseo.ac.kr

Published online: 24 December 2014; AJC-16441

$NaY_{1-x}(WO_4)_2$:Ho^{3+}/Yb^{3+} phosphors with doping concentrations of Ho^{3+} and Yb^{3+} (x = Ho^{3+} + Yb^{3+}, Ho^{3+} = 0.05, 0.1, 0.2 and Yb^{3+} = 0.2, 0.45) were successfully synthesized by the cyclic microwave-modified sol-gel process and their upconversion properties were investigated. Well-crystallized particles showed a fine and homogeneous morphology with particle sizes of 2-5 μm. Under excitation at 980 nm, the synthesized particles exhibited yellow emissions based on a strong 550 nm emission band and a strong 655 nm emission band in the red region. The Raman spectra of the doped particles indicated the domination of strong peaks at higher frequencies and weak peaks at lower frequencies induced by the disorder of the $[WO_4]^{2-}$ groups with the incorporation of the Ho^{3+} and Yb^{3+} elements into the crystal lattice or by a new phase formation.

Keywords: Microwave sol-gel, Yellow emission, Upconversion, Raman spectroscopy.

INTRODUCTION

Photoluminescence particles have evolved in their applications, such as fluorescent lamps, cathode ray tubes, solid-state laser, amplifiers for fiber optics communication and new optoelectronic devices, which show high luminescence quantum yields, since usually more than one metastable excited state exists, multiple emissions are observed[1-3]. The double tungstates of $MR(WO_4)_2$ (M = Li^+, Na^+, K^+; R = La^{3+}, Gd^{3+}, Y^{3+}) possess the tetragonal scheelite structure with the space group $I4_{1/a}$ and belong to the family of double tungstates compounds. It is possible for the trivalent rare-earth ions in the disordered tetragonal-phase to be partially substituted by Ho^{3+} and Yb^{3+} ions. These ions are effectively doped into the crystal lattices of the tetragonal phase due to the similar radii of the trivalent rare-earth ions in R^{3+}. This results in high red emitting efficiency and superior thermal and chemical stability. In these compounds, W^{6+} is coordinated by four O^{2-} at a tetrahedral site, which makes $[WO_4]^{2-}$ relatively stable. R^{3+} and M^+ are randomly distributed over the same cationic sublattice and they are coordinated by eight O^{2-} from near four $[WO_4]^{2-}$ with a symmetry S_4 without an inversion center[4,5]. The $[WO_4]^{2-}$ group has strong absorption in the near ultraviolet region, so that energy transfers process from $[WO_4]^{2-}$ group to rare-earth ions can easily occur, which can greatly enhance the external quantum efficiency of rare-earth ions doped materials. Among rare earth ions, the Ho^{3+} ion is suitable for converting infrared to visible light through the upconversion process due to its appropriate electronic energy level configuration. The co-doped Yb^{3+} ion and Ho^{3+} ion can remarkably enhance the upconversion efficiency for the shift from infrared to visible light due to the efficiency of the energy transfer from Yb^{3+} to Ho^{3+}. The Yb^{3+} ion, as a sensitizer, can be effectively excited by an incident light source energy. This energy is transferred to the activator from which radiation can be emitted. The Ho^{3+} ion activator is the luminescence center of the upconversion particles, while the sensitizer Yb^{3+} enhances the upconversion luminescence efficiency[6,7].

$NaY(WO_4)_2$:Ho^{3+}/Yb^3 phosphors have been developed to prepare including solid-state reactions[8,9], the hydrothermal method[10], the Czochralski method[11]. Compared with the usual methods, microwave synthesis has the advantages of a very short reaction time, small-size particles, narrow particle size distribution and high purity of final polycrystalline samples. Microwave heating is delivered to the material surface by radiant and/or convection heating, which is transferred to the bulk of the material *via* conduction[12]. A microwave-modified sol-gel process is a cost-effective method that provides high homogeneity and is easy to scale-up and it is emerging as a viable alternative approach for the quick synthesis of high-

quality luminescent materials. However, the synthesis of $NaY(WO_4)_2$:Ho^{3+}/Yb^3 phosphors by the microwave-modified sol-gel process has not been reported.

In this study, $NaY_{1-x}(WO_4)_2$:Ho^{3+}/Yb^{3+} phosphors with doping concentrations of Ho^{3+} and Yb^{3+} (x = Ho^{3+} + Yb^{3+}, Ho^{3+} = 0.05, 0.1, 0.2 and Yb^{3+} = 0.2, 0.45) phosphors were prepared by the cyclic microwave-modified sol-gel process followed by heat treatment. The synthesized particles were characterized by X-ray diffraction (XRD), scanning electron microscopy (SEM) and energy-dispersive X-ray spectroscopy (EDS). The optical properties were examined comparatively using photoluminescence (PL) emission and Raman spectroscopy.

EXPERIMENTAL

Appropriate stoichiometric amounts of $Na_2WO_4{\cdot}2H_2O$ (99 %, Sigma-Aldrich, USA), $Y(NO_3)_3{\cdot}6H_2O$ (99 %, Sigma-Aldrich, USA), $(NH_4)_6W_{12}O_{39}{\cdot}xH_2O$ (99 %, Alfa Aesar, USA), $Ho(NO_3)_3{\cdot}5H_2O$ (99.9 %, Sigma-Aldrich, USA), $Yb(NO_3)_3{\cdot}5H_2O$ (99.9 %, Sigma-Aldrich, USA), citric acid (99.5 %, Daejung Chemicals, Korea), NH_4OH (A.R.), ethylene glycol (A.R.) and distilled water were used to prepare $NaY(WO_4)_2$, $NaY_{0.8}(WO_4)_2$:$Ho_{0.2}$, $NaY_{0.7}(WO_4)_2$:$Ho_{0.1}Yb_{0.2}$ and $NaY_{0.5}(WO_4)_2$:$Ho_{0.05}Yb_{0.45}$ compounds with doping concentrations of Ho^{3+} and Yb^{3+} (Ho^{3+} = 0.05, 0.1, 0.2 and Yb^{3+} = 0.2, 0.45). To prepare $NaY(WO_4)_2$, 0.2 mol % $Na_2WO_4{\cdot}2H_2O$ and 0.067 mol % $(NH_4)_6W_{12}O_{39}{\cdot}xH_2O$ were dissolved in 20 mL of ethylene glycol and 80 mL of 5 M NH_4OH under vigorous stirring and heating. Subsequently, 0.4 mol % $Y(NO_3)_3{\cdot}6H_2O$ and citric acid (with a molar ratio of citric acid to total metal ions of 2:1) were dissolved in 100 mL of distilled water under vigorous stirring and heating. Then, the solutions were mixed together under vigorous stirring and heating at 80-100 °C. At the end, highly transparent solutions were obtained and adjusted to pH = 7-8 by the addition of NH_4OH or citric acid. In order to prepare $NaY_{0.8}(W\text{-}O_4)_2$:$Ho_{0.2}$, the mixture of 0.32 mol % $Y(NO_3)_3{\cdot}6H_2O$ with 0.08 mol % $Ho(NO_3)_3{\cdot}5H_2O$ was used for the creation of the rare-earth solution. In order to prepare $NaY_{0.7}(WO_4)_2$:$Ho_{0.1}Yb_{0.2}$, the mixture of 0.28 mol % $Y(NO_3)_3{\cdot}6H_2O$ with 0.04 mol % $Ho(NO_3)_3{\cdot}5H_2O$ and 0.08 mol % $Yb(NO_3)_3{\cdot}5H_2O$ was used for the creation of the rare-earth solution. In order to prepare $NaY_{0.5}(WO_4)_2$:$Ho_{0.05}Yb_{0.45}$, the rare-earth containing solution was generated using 0.2 mol % $Y(NO_3)_3{\cdot}6H_2O$ with 0.02 mol % $Ho(NO_3)_3{\cdot}5H_2O$ and 0.18 mol % $Yb(NO_3)_3{\cdot}5H_2O$.

The transparent solutions were placed into a microwave oven operating at a frequency of 2.45 GHz with a maximum output-power of 1250 W for 0.5 h. The working cycle of the microwave reaction was controlled very precisely using a regime of 40 s on and 20 s off for 15 min, followed by further treatment of 30 s on and 30 s off for 15 min. The samples were treated with ultrasonic radiation for 10 min to produce a light yellow transparent sol. After this, the light yellow transparent sols were dried at 120 °C in a dry oven to obtain black dried gels. The black dried gels were grinded and treated at 900 °C for 16 h with 100 °C intervals between 600-900 °C. Finally, white particles were obtained for $NaY(WO_4)_2$ and pink particles for the doped compositions.

The phase composition of the synthesized particles was identified using XRD (D/MAX 2200, Rigaku, Japan). The microstructure and surface morphology of the synthesized particles were observed using SEM/EDS (JSM-5600, JEOL, Japan). The photoluminescence spectra were recorded using a spectrophotometer (Perkin Elmer LS55, UK) at room temperature. Raman spectroscopy measurements were performed using a LabRam Aramis (Horiba Jobin-Yvon, France). The 514.5 nm line of an Ar ion laser was used as the excitation source and the power on the samples was kept at 0.5 mW.

RESULTS AND DISCUSSION

Fig. 1 shows the X-ray diffraction patterns of the (a) JCPDS 48-0886 data of $NaY(WO_4)_2$, the synthesized (b) $NaY(WO_4)_2$, (c) $NaY_{0.8}(WO_4)_2$:$Ho_{0.2}$, (d) $NaY_{0.7}(WO_4)_2$:$Ho_{0.1}Yb_{0.2}$ and (e) $NaY_{0.5}(WO_4)_2$:$Ho_{0.05}Yb_{0.45}$ particles. All of the XRD peaks could be assigned to the tetragonal-phase $NaY(WO_4)_2$ with the space group of $I4_1/a$, which was in good agreement with the crystallographic data of $NaY(WO_4)_2$ (JCPDS 48-0886). No impurity phases were detected. This finding means that the tetralgonal-phase $NaY_{1-x}(WO_4)_2$:Ho^{3+}/Yb^{3+} particles can be prepared by the cyclic microwave-modified sol-gel process. Post heat-treatment plays an important role in a well-defined crystallized morphology. To achieve a well-defined crystalline morphology, $NaY(WO_4)_2$, $NaY_{0.8}(WO_4)_2$:$Ho_{0.2}$, $NaY_{0.7}(WO_4)_2$:$Ho_{0.1}Yb_{0.2}$ and $NaY_{0.5}(WO_4)_2$:$Ho_{0.05}Yb_{0.45}$ phases need to be heat treated at 900 °C for 16 h. It is assumed that the doping amount of Ho^{3+}/Yb^{3+} has a great effect on the crystalline cell volume of the $NaY(WO_4)_2$, because of the different ionic sizes and energy band gaps. This means that the obtained samples possess a tetragonal-phase after partial substitution of Y^{3+} by Ho^{3+} and Yb^{3+} ions and the ions are effectively doped into crystal lattices of the $NaY(WO_4)_2$ phase due to the similar radii of Y^{3+}, Ho^{3+} and Yb^{3+}.

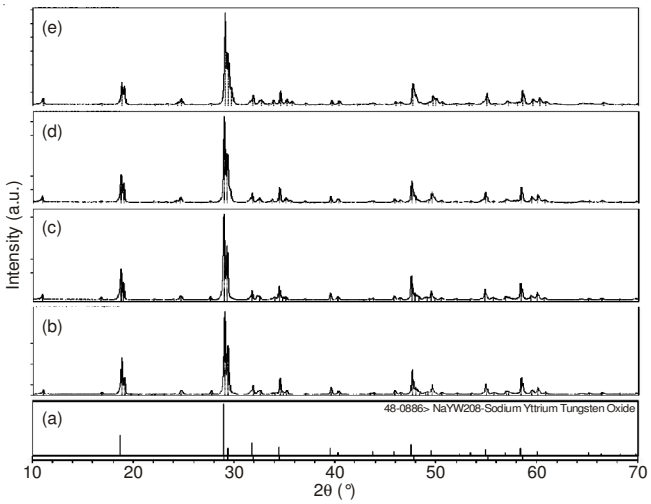

Fig. 1. X-ray diffraction patterns of the (a) JCPDS 48-0886 data of $NaY(WO_4)_2$, the synthesized (b) $NaY(WO_4)_2$, (c) $NaY_{0.8}(WO_4)_2$:$Ho_{0.2}$, (d) $NaY_{0.7}(WO_4)_2$:$Ho_{0.1}Yb_{0.2}$, and (e) $NaY_{0.5}(WO_4)_2$:$Ho_{0.05}Yb_{0.45}$ particles

Fig. 2 shows a SEM image of the synthesized $KGd_{0.5}(WO_4)_2$:$Ho_{0.05}Yb_{0.45}$ particles. The as-synthesized samples are well crystallized with a fine and homogeneous morphology and particle size of 2-5 μm. Fig. 3 shows the energy-dispersive X-ray spectroscopy patterns of the synthesized (a) $NaY_{0.8}(WO_4)_2$:$Ho_{0.2}$

and (b) $NaY_{0.5}(WO_4)_2$:$Ho_{0.05}Yb_{0.45}$ particles and quantitative compositions of (c) $NaY_{0.8}(WO_4)_2$:$Ho_{0.2}$ and (d) $KNaY_{0.5}(WO_4)_2$:$Ho_{0.05}Yb_{0.45}$ particles. The EDS pattern shows that the (a) $NaY_{0.8}(WO_4)_2$:$Ho_{0.2}$ and (b) $NaY_{0.5}(WO_4)_2$: $Ho_{0.05}Yb_{0.45}$ particles are composed of Na, Y, W, O and Ho for $NaY_{0.8}(WO_4)_2$:$Ho_{0.2}$ and Na, Y, W, O, Ho and Yb for $NaY_{0.5}(W\text{-}O_4)_2$:$Ho_{0.05}Yb_{0.45}$ particles. The quantitative compositions of (c) and (d) are in good relation with nominal compositions of the particles. The relation of Na, Y, W, O, Ho and Yb components exhibit that $NaY_{0.8}(WO_4)_2$:$Ho_{0.2}$ and $NaY_{0.5}(WO_4)_2$: $Ho_{0.05}Yb_{0.45}$ particles can be successfully synthesized by the cyclic microwave-modified sol-gel process. The cyclic microwave-modified sol-gel process of double tungstates provides the energy to synthesize the bulk of the material uniformly, so that the fine particles with controlled morphology can be fabricated in a short time period. The method is a cost-effective way to provide highly homogeneous products and is easy to scale-up, it is a viable alternative for the rapid synthesis of upconversion particles.

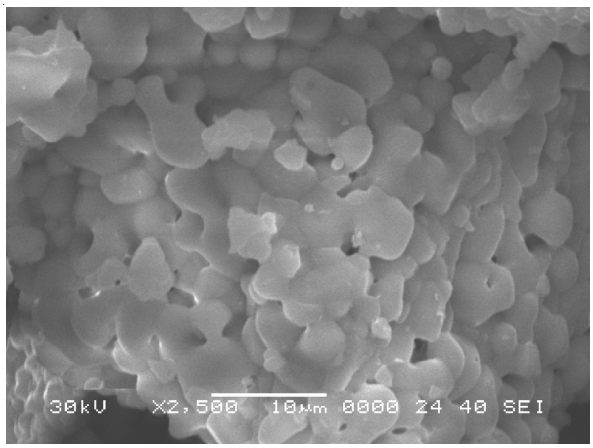

Fig. 2. Scanning electron microscopy image of the synthesized $NaY_{0.5}(WO_4)_2$:$Ho_{0.05}Yb_{0.45}$ particles

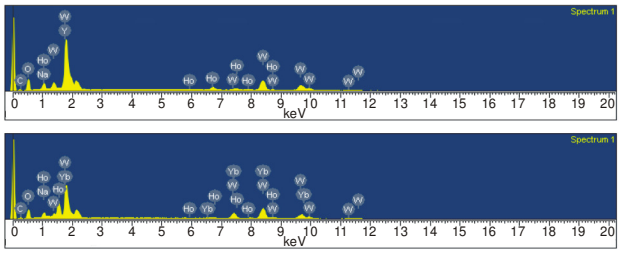

(c)

Spectrum	In stats.	C	O	Na	Y	Ho	W	Total
Spectrum 1	Yes	7.01	29.34	2.87	12.62	7.71	40.45	100.00
Spectrum 2	Yes	5.45	29.27	3.10	12.67	8.14	41.37	100.00
Spectrum 3	Yes	6.69	28.69	3.07	13.11	7.60	40.85	100.00
Spectrum 4	Yes	9.13	29.35	2.71	11.32	8.37	39.12	100.00
Mean		7.07	29.16	2.94	12.43	7.96	40.45	100.00
Std. deviation		1.53	0.32	0.18	0.77	0.36	0.96	
Max.		9.13	29.35	3.10	13.11	8.37	41.37	
Min.		5.45	28.69	2.71	11.32	7.60	39.12	

(d)

Spectrum	In stats.	C	O	Na	Ho	Yb	W	Total
Spectrum 1	Yes	8.46	26.40	2.61	2.21	23.58	36.73	100.00
Spectrum 2	Yes	7.57	26.97	2.52	2.07	23.51	37.36	100.00
Spectrum 3	Yes	9.12	26.90	2.51	2.64	23.26	35.56	100.00
Spectrum 4	Yes	7.02	27.32	2.79	1.98	23.45	37.44	100.00
Mean		8.04	26.90	2.61	2.23	23.45	36.77	100.00
Std. deviation		0.93	0.38	0.13	0.29	0.14	0.87	
Max.		9.12	27.32	2.79	2.64	23.58	37.44	
Min.		7.02	26.40	2.51	1.98	23.26	35.56	

Fig. 3. Energy-dispersive X-ray spectroscopy patterns of the synthesized (a) $NaY_{0.8}(WO_4)_2$:$Ho_{0.2}$ and (b) $NaY_{0.5}(WO_4)_2$:$Ho_{0.05}Yb_{0.45}$ particles, and quantitative compositions of (c) $NaY_{0.8}(WO_4)_2$:$Ho_{0.2}$ and (d) $NaY_{0.5}(WO_4)_2$:$Ho_{0.05}Yb_{0.45}$ particles

Fig. 4 shows the upconversion photoluminescence emission spectra of the as-prepared (a) $NaY(WO_4)_2$, (b) $NaY_{0.8}(WO_4)_2$:$Ho_{0.2}$, (c) $NaY_{0.7}(WO_4)_2$:$Ho_{0.1}Yb_{0.2}$ and (d) $NaY_{0.5}(WO_4)_2Ho_{0.05}Yb_{0.45}$ particles excited under 980 nm at room temperature. The upconversion intensities of (a) $NaY(WO_4)_2$ and (b) $NaY_{0.8}(WO_4)_2$:$Ho_{0.2}$ were not detected. The upconversion intensities of (c) $NaY_{0.7}(WO_4)_2$:$Ho_{0.1}Yb_{0.2}$ and (d) $NaY_{0.5}(WO_4)_2Ho_{0.05}Yb_{0.45}$ particles exhibited yellow emissions based on a strong 550 nm emission band in the green region and a strong 655 nm emission band in the red region. The upconversion intensity of $NaY_{0.5}(WO_4)_2Ho_{0.05}Yb_{0.45}$ particles was higher than that of the $NaY_{0.7}(WO_4)_2$:$Ho_{0.1}Yb_{0.2}$ particles. The strong 550 nm emission band in the green region correspond to the $^5S_2/^5F_4 \rightarrow {}^5I_8$ transition, while the strong emission 655 nm band in the red region corresponds to the $^5F_5 \rightarrow {}^5I_8$ transferred to the activator where radiation can be emitted. The Ho^{3+} ion activator is the luminescence center for these upconversion particles and the sensitizer Yb^{3+} enhances the upconversion luminescence efficiency.

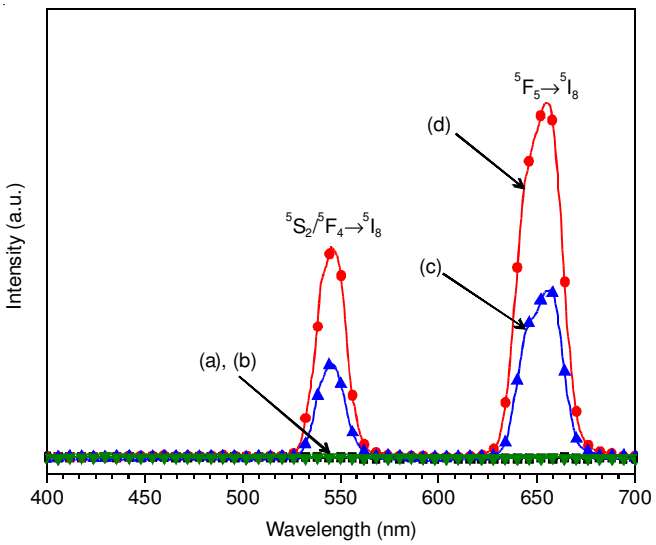

Fig. 4. Upconversion photoluminescence emission spectra of (a) $NaY(WO_4)_2$, (b) $NaY_{0.8}(WO_4)_2$:$Ho_{0.2}$, (c) $NaY_{0.7}(WO_4)_2$:$Ho_{0.1}Yb_{0.2}$ and (d) $NaY_{0.5}(WO_4)2Ho_{0.05}Yb_{0.45}$ particles excited under 980 nm at room temperature

Fig. 5 shows schematic energy level diagrams of Ho^{3+} ions (activator) and Yb^{3+} ions (sensitizer) in the as-prepared $NaY_{1-x}(WO_4)_2$:Ho^{3+}/Yb^{3+} samples and the upconversion mechanisms accounting for the green and red emissions during 980 nm laser excitation. The upconversion emissions are generated by a two photon process through excited state absorption (ESA) and energy transfer (ET). Initially, the Yb^{3+} ion sensitizer is excited from the $^2F_{7/2}$ level to the $^4F_{5/2}$ level under excitation of 980 nm pumping and transfers its energy to Ho^{3+} ions. Then Ho^{3+} ions is populated from the $^5I_8$ ground state to $^5I_6$ excited state. This is a phonon-assisted energy transfer process because of energy mismatch between $^2F_{5/2}$ level of Yb^{3+} and $^5I_6$ level of Ho^{3+}. Secondly, the Ho^{3+} in $^5I_6$ level is excited to $^5S_2$ or $^5F_4$ level by the same energy transfer from Yb^{3+}. In addition, the $^5S_2/^5F_4$ level of Ho^{3+} can also populated through excited state absorption. Finally, the green emission around 550 nm corresponding to $^5S_2/^5F_4 \rightarrow {}^5I_8$ transition takes place. For red emission, the population of the $^5F_5$ level is generated by two different channels.

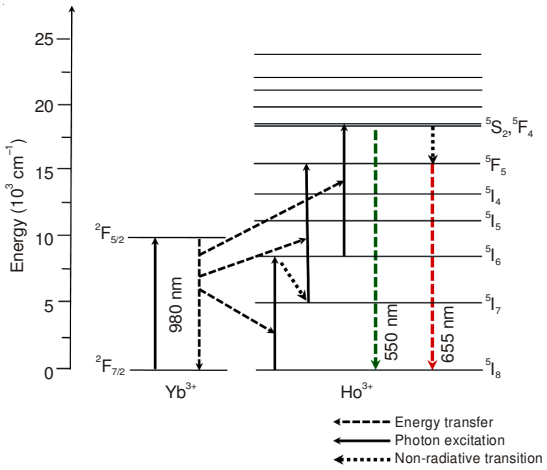

Fig. 5. Schematic energy level diagrams of Ho^{3+} ions (activator) and Yb^{3+} ions (sensitizer) in the as-prepared $NaY_{1-x}(WO_4)_2$:Ho^{3+}/Yb^{3+} system and the upconversion mechanisms accounting for the green and red emissions under 980 nm laser excitation

One channel is that Ho^{3+} in the $^5S_2$/$^5F_4$ level relaxes non-radiatively to the $^5F_5$ level. Another channel is closely related to the $^5I_7$ level populated by non-radiative relaxation from the $^5I_6$ excited state. The Ho^{3+} in $^5I_7$ level is excited to the $^5F_5$ level by the energy transfer from Yb^{3+}. Therefore, the red emission around 655 nm is corresponding to the $^5F_5 \rightarrow {}^5I_8$ transition[13,14].

Fig. 6 shows the Raman spectra of the synthesized (a) $NaY(WO_4)_2$(NYW), (b) $NaY_{0.8}(WO_4)_2$:$Ho_{0.2}$ NYW:Ho), (c) $NaY_{0.7}(WO_4)_2$:$Ho_{0.1}Yb_{0.2}$(NYW:HoYb) and (d) $NaY_{0.5}(WO_4)_2$:$Ho_{0.05}Yb_{0.45}$ (NYW:HoYb#) particles excited by the 514.5 nm line of an Ar ion laser at 0.5 mW. The well-resolved sharp peaks for the (a) $NaY(WO_4)_2$ particles indicate a high crystallinity state of the synthesized particles. The internal vibration mode frequencies are dependent on the lattice parameters and the degree of the partially covalent bond between the cation and molecular ionic group $[WO_4]^{2-}$. The Raman spectra of the (b) $NaY_{0.8}(WO_4)_2$:$Ho_{0.2}$ NYW:Ho), (c) $NaY_{0.7}(WO_4)_2$: $Ho_{0.1}Yb_{0.2}$ (NYW:HoYb) and (d) $NaY_{0.5}(WO_4)_2$:$Ho_{0.05}Yb_{0.45}$ (NYW:HoYb#) particles indicate the domination of strong peaks at higher frequencies of 812, 840, 926, 938, 1111 and 1265 cm^{-1} and weak peaks at lower frequencies of 274, 310 and 334 cm^{-1}. The Raman

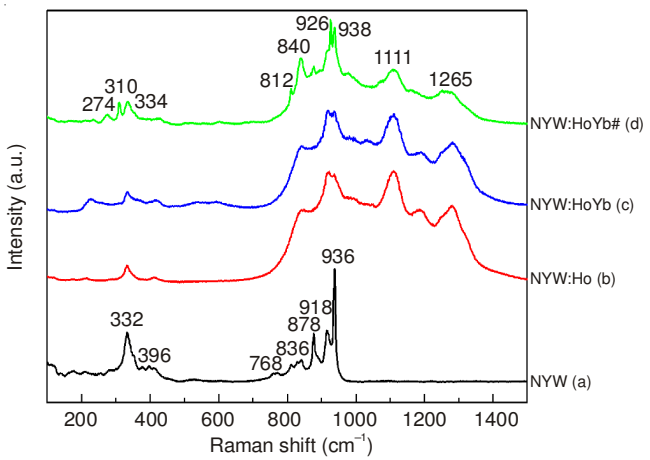

Fig. 6. Raman spectra of the synthesized (a) $NaY(WO_4)_2$(NYW), (b) $NaY_{0.8}(WO_4)_2$:$Ho_{0.2}$ NYW:Ho), (c) $NaY_{0.7}(WO_4)_2$:$Ho_{0.1}Yb_{0.2}$ (NYW: HoYb) and (d) $NaY_{0.5}(WO_4)_2$:$Ho_{0.05}Yb_{0.45}$ (NYW:HoYb#) particles excited by the 514.5 nm line of an Ar ion laser at 0.5 mW

spectra of the doped particles prove that the doping ions can influence the structure of the host materials. The combination of a heavy metal cation and the large inter-ionic distance for Ho^{3+} and Yb^{3+} substitutions in Y^{3+} sites in the lattice result in a high probability of upconversion and phonon-splitting relaxation in $KGd_{1-x}(WO_4)_2$ crystals. It is noted that these very strong and strange effects are generated by the disorder of the $[WO_4]^{2-}$ groups with the incorporation of the Ho^{3+} and Yb^{3+} elements into the crystal lattice or by a new phase formation.

Conclusion

The double tungstate $NaY_{1-x}(WO_4)_2$:Ho^{3+}/Yb^{3+} phosphors with doping concentrations of Ho^{3+} and Yb^{3+} (x = Ho^{3+} + Yb^{3+}, Ho^{3+} = 0.05, 0.1, 0.2 and Yb^{3+} = 0.2, 0.45) were successfully synthesized by the cyclic microwave-modified sol-gel process. Well-crystallized particles formed after heat-treatment at 900 °C for 16 h showed a fine and homogeneous morphology with particle sizes of 2-5 μm. Under excitation at 980 nm, the upconversion intensities of $NaY_{0.7}(WO_4)_2$:$Ho_{0.1}Yb_{0.2}$ and $NaY_{0.5}(WO_4)_2$: $Ho_{0.05}Yb_{0.45}$ particles exhibited yellow emissions based on a strong 550 nm emission band in the green region and a strong 655 nm emission band in the red region, which were assigned to the $^5S_2$/$^5F_4 \rightarrow {}^5I_8$ and $^5F_5 \rightarrow {}^5I_8$ transitions, respectively. The upconversion intensity of $NaY_{0.5}(WO_4)_2Ho_{0.05}Yb_{0.45}$ particles was higher than that of the $NaY_{0.7}(WO_4)_2$:$Ho_{0.1}Yb_{0.2}$ particles. The Raman spectra of the doped particles indicated the domination of strong peaks at higher frequencies of 812, 840, 926, 938, 1111 and 1265 cm^{-1} and weak peaks at lower frequencies of 274, 310 and 334 cm^{-1} induced by the disorder of the $[WO_4]^{2-}$ groups with the incorporation of the Ho^{3+} and Yb^{3+} elements into the crystal lattice or by a new phase formation.

ACKNOWLEDGEMENTS

This study was supported by the Basic Science Research Program through the National Research Foundation of Korea (NRF) funded by the Ministry of Science, ICT & Future Planning (2014-046024).

REFERENCES

1. M. Wang, G. Abbineni, A. Clevenger, C. Mao and S. Xu, *Nanomedicine*, **7**, 710 (2011).
2. Y.J. Chen, H.M. Zhu, Y.F. Lin, X.H. Gong, Z.D. Luo and Y.D. Huang, *Opt. Mater.*, **35**, 1422 (2013).
3. M. Lin, Y. Zhao, S.Q. Wang, M. Liu, Z.F. Duan, Y.M. Chen, F. Li, F. Xu and T.J. Lu, *Bio. Adv.*, **30**, 1551 (2012).
4. L. Li, L. Liu, W. Zi, H. Yu, S. Gan, G. Ji, H. Zou and X. Xu, *J. Lumin.*, **143**, 14 (2013).
5. C. Ming, F. Song and L. Yan, *Opt. Commun.*, **286**, 217 (2013).
6. W. Liu, J. Sun, X. Li, J. Zhang, Y. Tian, S. Fu, H. Zhong, T. Liu, L. Cheng, H. Zhong, H. Xia, B. Dong, R. Hua, X. Zhang and B. Chen, *Opt. Mater.*, **35**, 1487 (2013).
7. W. Xu, H. Zhao, Y. Li, L. Zheng, Z. Zhang and W. Cao, *Sens. Actuators B*, **188**, 1096 (2013).
8. X. Liu, W. Xiang, F. Chen, W. Zhang and Z. Hu, *Mater. Res. Bull.*, **47**, 3417 (2012).
9. X. Liu, W. Xiang, F. Chen, Z. Hu and W. Zhang, *Mater. Res. Bull.*, **48**, 281 (2013).
10. S. Huang, D. Wang, Y. Wang, L. Wang, X. Zhang and P. Yang, *J. Alloys Comp.*, **529**, 140 (2012).
11. J. Feng, J. Xu, Z. Zhu, Y. Wang, Z. You, J. Li, H. Wang and C. Tu, *J. Alloys Comp.*, **566**, 229 (2013).
12. C.S. Lim, *Mater. Res. Bull.*, **47**, 4220 (2012).
13. Y. Xu, Y. Wang, L. Shi, L. Xing and X. Tan, *Opt. Laser Technol.*, **54**, 50 (2013).
14. X. Li, Q. Nie, S. Dai, T. Xu, L. Lu and X. Zhang, *J. Alloys Comp.*, **454**, 510 (2008).